EC
Journals.ASM.org

F-Box Protein RcyA Controls Turnover of the Kinesin-7 Motor KipA in *Aspergillus nidulans*

Saturnino Herrero,[a] Norio Takeshita,[a,b] Reinhard Fischer[a]

Karlsruhe Institute of Technology (KIT), Institute for Applied Biosciences, Dept. of Microbiology, Karlsruhe, Germany[a]; University of Tsukuba, Faculty of Life and Environmental Sciences, Tsukuba, Ibaraki, Japan[b]

Fungal filamentous growth depends on continuous membrane insertion at the tip, the delivery of membrane-bound positional markers, and the secretion of enzymes for cell wall biosynthesis. This is achieved through exocytosis. At the same time, polarized growth requires membrane and protein recycling through endocytosis. Endocytic vesicles are thought to enter the protein degradation pathway or recycle their content to the cell surface. In *Saccharomyces cerevisiae*, the Rcy1 F-box protein is involved in the recycling process of a v-SNARE protein. We identified a Rcy1 orthologue, RcyA, in the filamentous fungus *Aspergillus nidulans* as a protein interacting with the KipA kinesin-7 motor protein in a yeast two-hybrid screen. The interaction was confirmed through bimolecular fluorescence complementation. RcyA possesses an F-box domain at the N terminus and a prenylation (CaaX) motif at the C terminus. RcyA shows also similarity to Sec10, a component of the exocyst complex. The RcyA protein localized to the hyphal tip and forming septa, likely through transportation on secretory vesicles and partially on early endosomes, but independently of KipA. Deletion of *rcyA* did not cause severe morphological changes but caused partial defects in the recycling of the SynA v-SNARE protein and the positioning of the cell end markers TeaA and TeaR. In addition, deletion of *rcyA* led to increased concentrations of the KipA protein, whereas the transcript concentration was unaffected. These results suggest that RcyA probably labels KipA for degradation and thereby controls the protein amount of KipA.

During cellular growth and reproduction, the concentration of many cellular components needs to be increased. However, certain cellular components are required only during certain stages or for special events and thus the turnover of such components needs to be strictly regulated (1). Specific labeling of proteins for degradation occurs through covalent labeling of small modifiers such as ubiquitin. Polyubiquitination depends on E3 ubiquitin ligases in the anaphase-promoting complex/cyclosome (APC/C) or the Skp/Cullin/F-box (SCF) complex. Polyubiquitination allows recognition and subsequent proteolysis of the substrate proteins by the 26S proteasome (1). The core of the SCF complex is formed by Skp1, Rbx1, and cullin (Cul1) as a scaffold protein. Rbx1 resides in the catalytic part of the complex and binds to the ubiquitin ligase, whereas Skp1 interacts with the F-box domain of different proteins. F-box proteins are specific adaptors to E3 ligases and determine the fate of different substrate proteins. The number of F-box proteins ranges from 20 in *Saccharomyces cerevisiae* to more than 70 in humans. A similar number of F-box proteins was reported in *Aspergillus nidulans*, 42 of which have already been studied to some extent and play a role in cellular differentiation and sexual development (2–4).

Another function of ubiquitination is related to the recycling of membranes. As an alternative to the cytoplasmic proteasome, monoubiquitination leads to protein degradation through the vacuole/lysosome pathway. Monoubiquitination can also be a signal for membrane protein trafficking, sorting of transmembrane proteins, regulation of transcription factors, and posttranslational histone modifications (5). A protein involved in the recycling of membrane proteins in *S. cerevisiae* is the F-box protein Rcy1 (6). Rcy1 regulates the endosome-Golgi transport by ubiquitination of recycling proteins, specifically, the recycling of the v-SNARE protein synaptobrevin (Snc1) to a nondegradative (Golgi) compartment. Snc1 is recycled from the Golgi compartment to the plasma membrane via secretory vesicles. Deletion of *rcy1* leads to an accumulation of Snc1 at early endosomes and causes a cold-sensitive growth defect. Rcy1 is an effector of the Rab GTPase Ypt31/32 and is also necessary for the recycling of the subtilisin-like protease Kex2 and the phopholipid translocase Cdc50/Drs2 (7, 8). In contrast, the Rcy1 orthologue in *Schizosaccharomyces pombe*, Pof6, is involved in cell separation and is essential for viability (9). The role of Pof6 and Skp1 in cell separation is unclear, but it was speculated that it could involve the exocyst complex. Moreover, it was proposed that Rcy1/Pof6 forms a non-SCF complex with Skp1 during v-SNARE recycling, but more recent studies have shown reduced ubiquitination of Snc1 in *rcy1*Δ mutants and an accumulation of (nonubiquitinable) Snc1-K63R in early endosomes, supporting the idea that Rcy1/Skp1 is part of a functional ubiquitin-ligase complex (10).

Growth in filamentous fungi depends on the continuous flow of vesicles, which deliver enzymes for cell wall biosynthesis to the growing tip (11). In addition, subapical endocytosis is required for recycling of excess membrane and membrane-bound proteins (12–15). The direction of vesicle flow is strictly regulated through the orientation and polarization of the microtubule and the actin cytoskeletons. Vesicles can be transported along either cytoskeleton for specific purposes. Whereas microtubules are necessary for long-distance transportation of excocytic vesicles and endosomes, actin serves as track for short-distance transportation of secretory

Received 20 February 2014 **Accepted** 13 June 2014
Published ahead of print 20 June 2014
Address correspondence to Reinhard Fischer, reinhard.fischer@KIT.edu.
Supplemental material for this article may be found at http://dx.doi.org/10.1128/EC.00042-14.

doi:10.1128/EC.00042-14

vesicles prior to fusion with the membrane. In *Aspergillus nidulans*, close to the growing tip, almost all microtubules are oriented with their plus ends toward the tip, whereas actin filaments have their origin at the tip membrane. This organization is achieved through interplay between the two cytoskeletons through the activity of a class of proteins named cell end markers (16, 17). They were discovered in *S. pombe* and were characterized afterward in *A. nidulans* (17–20). Cell end markers are transported through microtubules to the tip, are tethered to the membrane through a prenyl anchor, and form a protein complex. One of the protein complex proteins in *A. nidulans* is the formin SepA. Why the cell end markers remain at the very tip, although continuous membrane insertion should cause their diffusion along the membrane, is still an open issue.

In this work, we report on the characterization of RcyA, the *A. nidulans* orthologue of Rcy1 and Pof6. In the filamentous fungus, RcyA appears to be involved in membrane recycling through recycling of v-SNARE, which is necessary for the positioning of cell end markers. In addition, RcyA controls the concentration of the kinesin-7 motor protein KipA, suggesting KipA as a novel target of RcyA.

MATERIALS AND METHODS

Strains, plasmids, and culture conditions. Supplemented minimal media (MM) for *A. nidulans* were prepared as described, and standard strain construction procedures were performed as previously described (21). A list of *A. nidulans* strains used in this study is given in Table 1. Standard laboratory *Escherichia coli* strains (XL-1 blue and Top 10 F′) were used. Plasmids are listed in Table 2.

Molecular techniques. Standard DNA transformation procedures were used for *A. nidulans* (31) and *E. coli* (32). For PCR experiments, standard protocols were applied using a Biometra Personal cycler (Biometra, Göttingen) for the reaction cycles. DNA sequencing was done commercially (eurofins-MWG-operon, Ebersberg, Germany). Genomic DNA was extracted from *A. nidulans* with an innuPREP Plant DNA kit (analytikjena, Jena, Germany). DNA analyses (Southern hybridizations) were performed as described in reference 32.

Deletion of *rcyA*. *rcyA* flanking regions were amplified by PCR using genomic DNA and primers rcyA-p3 (5′-AGGGTGAGCGCACAGCGAA-3′) and rcyA-p1 (5′-GAAGAGCATTGTTTGAGGCAATGTCTTTTCAAGGATTG-3′) for the upstream region of *rcyA* and rcyA-p5 (5′-ATCAGTGCCTCCTCTCAGACAGTGCAGCAACCGCTAATGTAT-3′) and rcyA-p8 (5′-CGTACAGAGTGCTTCCACTT-3′) for the downstream region. The *pyrG* gene from plasmid pFNO3 (S. Osmani) was amplified by PCR and used as the template together with *rcyA*-flanking regions for the fusion-PCR. The deletion cassette was amplified using the fusion-PCR method (33) and primers rcyA-p2 (5′-AGTCGAGAGTTCGAAGTCGT-3′) and rcyA-p7 (5′-AGTCTTTGGCATAGTCCGCA-3′). The resulting PCR product was transformed into *pyrG89*-auxotrophic *A. nidulans* strain TN02A3 (22), and transformants were selected and confirmed by Southern blotting (34).

Transformants were screened by PCR for the homologous integration event. Single integration of the construct was confirmed by Southern blotting. One *rcyA*-deletion strain was selected from the transformants and named SSH36.

Tagging of proteins with GFP. For fluorescence microscopy, a 0.7-kb fragment of the *rcyA* gene was subcloned in the pCMB17apx plasmid (28), where N-terminal fusions of green fluorescent protein (GFP) to proteins of interest are expressed under the control of the *alcA* promoter, containing *Neurospora crassa pyr-4* as a selection marker, yielding pSH13. GFP and *pyr-4* were replaced with mRFP1 and *pyroA*, yielding pSH30. The resulting plasmids are listed in Table 2. The primer set used for *rcyA* was AN10061-AscI (5′-GGCGCGCCTATGTCAAAAGCGAGGAATGGC-3′) and AN10061-PacI (5′-TTAATTAACGTAGTTCTTCATCGACCAT

TABLE 1 *A. nidulans* strains used in this study[a]

Strain	Genotype	Reference or source
TN02A3	*pyrG89 argB2 ΔnkuA::argB pyroA4*	22
RMS011	*pabaA1 yA2 ΔargB::trpCΔB trpC801 veA1*	23
SJW02	*wA3 pyroA4 alcA(p)-GFP-tubA ΔargB::trpCΔB*	J. Warmbold, Marburg, Germany
SSK44	*pabaA1 wA3 ΔargB::trpCΔB ΔkipA::pyr4 veA1*	24
SSK92	*wA3 pyroA4 alcA(p)-GFP-kipA*	24
SSK114	*pyrG89 ΔargB::trpCΔB pyroA4 veA1 alcA(p)-GFP-kipA^{rigor}::pyr-4*	24
LO1535	*fwA1 nicA2 pyrG89 pyroA4 ΔnkuA::argB synA(p)-GFP-synA*	25
SNT56	*pabaA1 teaA(p)-mRFP1-teaA teaR(p)-GFP-teaR*	19
SNZ14	*alcA(p)-GFP-uncA^{rigor} pyroA4*	26
SSH01	TN02A3 transformed with pSH13 [*alcA(p)-GFP-rcyA*]	This study
SSH08	SSK44 crossed with SSH01 [*ΔkipA alcA(p)-GFP-rcyA*]	This study
SSH14	TN02A3 transformed with pSH30 [*alcA(p)-mRFP1-rcyA pyrG89*]	This study
SSH27	*wA3 yA2 ΔargB::trpCΔB trpC801* [*alcA(p)-GFP-kipA*]	27
SSH36	*ΔrcyA::pyrG^{Af}* in TN02A3 *pyroA4*	This study
SSH37	SSK92 crossed with SSH14 [*alcA(p)-GFP-kipA alcA(p)-mRFP1-rcyA*]	This study
SSH43	SSH27 crossed with SSH36 [*alcA(p)-GFP-kipA ΔrcyA*]	This study
SSH44	SNT56 crossed with SSH36 [*ΔrcyA teaA(p)-mRFP1-teaA teaR(p)GFP-teaR*]	This study
SSH55	SNZ14 crossed with SSH14 [*alcA(p)-gfp-uncA^{rigor} alcA(p)-mRFP1-rcyA*]	This study
SSH56	LO1535 crossed with SSH14 [*synA(p)-GFP-synA alcA(p)-mRFP1-rcyA*]	This study
SSH66	SSK114 crossed with SSH14 [*alcA(p)-GFP-kipA^{rigor} alcA(p)-mRFP1-rcyA*]	This study
SSH67	TN02A3 transformed with pSH46 [*alcA(p)-mRFP1-rcyAΔF-box pyrG89*]	This study
SSH69	SSH67 crossed with SSH27 [*alcA(p)-mRFP1-rcyAΔF-box alcA(p)-GFP-kipA*]	This study
SSH73	TN02A3 transformed with pSH47 [*rcy(p)-GFP-rcyA pyroA4*]	This study
SSH89	SSH36 crossed with LO1535 [*ΔrcyA synA(p)-GFP-synA*]	This study
SSH91	SSK114 crossed with SSH14 [*alcA(p)-GFP-kinA^{rigor} alcA(p)-mRFP1-rcyA*]	This study
SCos135	TN02A3 transformed with p1789 [*alcA(p)-GFP-rabA pyrG89*]	C. Seidel, Karlsruhe, Germany
SNG67	SCos135 crossed with RMS011 [*alcA(p)-GFP-rabA pabaA1*]	This study
SSH93	SNG67 crossed with SSH14 [*alcA(p)-GFP-rabA alcA(p)-mRFP1-rcyA*]	This study

[a] All strains harbored the veA1 mutation in addition.

TABLE 2 List of plasmids used in this study

Plasmid	Description	Reference or source
pCMB17apx	*alcA(p)-GFP*, for N-terminal tagging of GFP to proteins of interest; contains *N. crassa pyr-4*	28
pDM8	GFP replaced mRFP1 in pCMB17apx	29
P1789	*alcA(p)-GFP-rabA*::*argB*	30
pSH13	*alcA(p)-GFP-rcyA*::*pyr-4*	This study
pSH30	*alcA(p)-mRFP1-rcyA*::*pyroA*^{Af}	This study
pSH46	*alcA(p)-mRFP1-rcyA*Δ*F-box*::*pyroA*^{Af}	This study
pSH47	*rcyA(p)-GFP-rcyA*::*pyr4*	This study

C-3′) (cloning sites are underlined). The ΔF box-deletion mutant was generated with the primers Delta-Fbox (5′-GGCGCGCCTAGGATAGG TTGCTGGGATGAAG-3′) and AN10061-PacI, and the PCR fragment was cloned into AscI-PacI-digested pSH30. All of these plasmids were transformed into the uracil-auxotrophic TN02A3 (Δ*nkuA*) strain (Table 1). The integration events were confirmed by PCR and Southern blotting.

Light/fluorescence microscopy. For live-cell imaging of germlings and young hyphae, cells were grown on coverslips in 0.4 ml MM plus 2% glycerol (derepression of the *alcA* promoter), MM plus 2% glucose (repression of the *alcA* promoter), or MM plus 2% threonine (induction of the *alcA* promoter) (35). Cells were incubated at room temperature overnight. Images were captured at room temperature using an Axiophot microscope (Zeiss, Jena, Germany). Images were collected and analyzed with the AxioVision system (Zeiss).

For FM4-64 staining, germlings were grown in MM plus 2% glucose medium overnight and stained with 0.3 ml medium containing 10 μM FM4-64 (from a stock solution in dimethyl sulfoxide [DMSO]), kept for 15 min, washed in 2.5 ml of medium, and transferred to 2.5 ml of fresh medium (36).

Real-time PCR (RT-PCR). For RNA isolation, mycelium was collected, shock-frozen in liquid nitrogen, and lyophilized. RNA was extracted with a Fungal RNA kit from Omega Bio-Tek following the manufacturer's protocol. RNA samples were obtained from TN02A3 (wild-type strain) and SSH36 (Δ*rcyA* strain). For DNA digestion, an Ambion Turbo DNA Free kit was used. For real-time PCR, a Bioline SensiFast SYBR kit and a Fluorescein One Step kit were used according to the manufacturer's protocol. Three technical replicates were performed. Histone H2B was taken as the housekeeping gene. *kipA* was amplified with primers RT-kipA-For (5′-GAGTGGATAGTGGATGCTCGTC-3′) and RT-kipA-Rev (5′-CCATCACCCTCCTTACCAAACG-3′). For normalization of the *kipA* transcript levels, histone 2B primers H2B-RT fwd (5′-CTGCCG AGAAGAAGCCTAGCAC-3′) and H2B-RT rev (5′-GAAGAGTAGGTC TCCTTCCTGGTC-3′) were used.

Western blotting. *A. nidulans* strains SSH27 (GFP-KipA) and SSH43 (GFP-KipA, Δ*rcyA*) were cultured in MM plus 2% glucose and strain SSH69 (GFP-KipA, mRFP1-RcyAΔF-box) in MM plus 2% threonine and 0.2% glucose for 24 h. The mycelium was ground in liquid nitrogen, resuspended in protein extraction buffer (50 mM Tris-HCl [pH 7.4], 150 mM NaCl, 5 mM EDTA), supplemented with a cocktail of protease inhibitor (Sigma), and centrifuged at 10,000 × *g* for 15 min. The supernatant (clarified cell lysate) and a MiniProtean system (Bio-Rad) were used for Western blotting following the manufacturer's instructions and a polyclonal anti-GFP antibody (Sigma) and a monoclonal anti gamma-tubulin antibody (Sigma) as internal controls for the basal protein amount. The signal intensities of the Western blotting bands were measured with a Chemi-Smart-5100 geldoc device (Peqlab) and quantified with the ChemiCap program (peqlab). The wild-type value was set to 100%. The experiment was repeated twice with three different amounts of total protein.

RESULTS

Identification of the RcyA F-box protein in a yeast two-hybrid screening with KipA as bait. In a yeast two-hybrid screening with the KipA kinesin-7 motor protein of *A. nidulans*, several interacting proteins were identified (27). One of the candidates characterized here was AN10061. The yeast two-hybrid clone spans 1.4 kb of a cDNA corresponding to a region close to the 3′ end of the gene (Fig. 1A). The complete cDNA comprises 2.6 kb and encodes a polypeptide of 880 amino acids, which shares 35% amino acid identity with Sls2 of *Yarrowia lipolytica* (37), 29% identity with Rcy1 of *S. cerevisiae* (6, 38), and 32.5% identity with Pof6 of *S. pombe* (9). In accordance with the budding yeast's name, we used the name *rcyA* for the *A. nidulans* gene. The *A. nidulans* RcyA polypeptide of between 100 to 850 amino acids also shares 25% identity and 40% similarity with exocyst complex component Sec10. In addition, RcyA contains an F-box domain at the N terminus. Sec10 is conserved in all eukaryotes, and the *A. nidulans* orthologue is AN8879 (39, 40). This *A. nidulans* Sec10 orthologue shares 24% identity and 39% similarity with the human Sec10 protein. At the extreme C terminus of RcyA, a putative prenylation motif (CaaX) was detected using the PrePS program (http://mendel.imp.ac.at/sat/PrePS/index.html). Proteins with these three features (similarity to Sec10, F-box proteins at the N terminus, and a CaaX motif at the C terminus) were found only in fungi, while Sec10 orthologues are present in all eukaryotes (Fig. 1B).

Localization of GFP-RcyA. In order to unravel the molecular function of RcyA, we studied the subcellular distribution of the protein. RcyA was fused to GFP at the N terminus and expressed from the endogenous promoter or the inducible promoter of the alcohol dehydrogenase (*alcA*) (35). With glucose as the carbon source, the promoter is repressed; with glycerol as the carbon source, it is derepressed and expressed at a low level; and with threonine or ethanol as the carbon source, high expression levels can be obtained. The localization pattern of GFP-RcyA expressed under the control of the endogenous promoter was similar to that of GFP-RcyA expressed under the control of the *alcA* promoter derepressed condition with glycerol as the carbon source. GFP-RcyA accumulated at the tip in a dynamic manner (Fig. 2A; see also Movie S1 in the supplemental material). The fluorescence signal sometimes moved back from the tip to a subapical region (Fig. 2A and B, arrows). Along hyphae, especially in regions further back, GFP-RcyA moved as small spots bidirectionally (Fig. 2C, arrowheads) and localized in larger accumulations close to the nuclei (Fig. 2B and C, arrows). The small spots moved at 2.0 μm/s on average (1.8 μm/s ± 0.5 μm/s standard deviation [SD]; $n = 10$) and at a maximum of 3.0 μm/s (Fig. 2C). GFP-RcyA also localized at forming septa (Fig. 2D, arrow) but not at mature septa (Fig. 2D, arrowhead).

RcyA transport. Because RcyA was identified as a kinesin-7-interacting protein by yeast two-hybrid screening (27), we anticipated that the dynamics of RcyA would depend on KipA. To test this hypothesis, we studied the localization of RcyA in the absence of KipA. However, no obvious difference from the wild type was observed. GFP-RcyA still accumulated at hyphal tips in the *kipA*-deletion strain and moved bidirectionally on small spots at a similar speed (Fig. 3A and data not shown). In addition, the signal of GFP-KipA at microtubule plus ends did not colocalize with that of mRFP1-RcyA (data not shown). In the case of KipA, a rigor version of the motor was used. Such rigor variants of kinesin bind

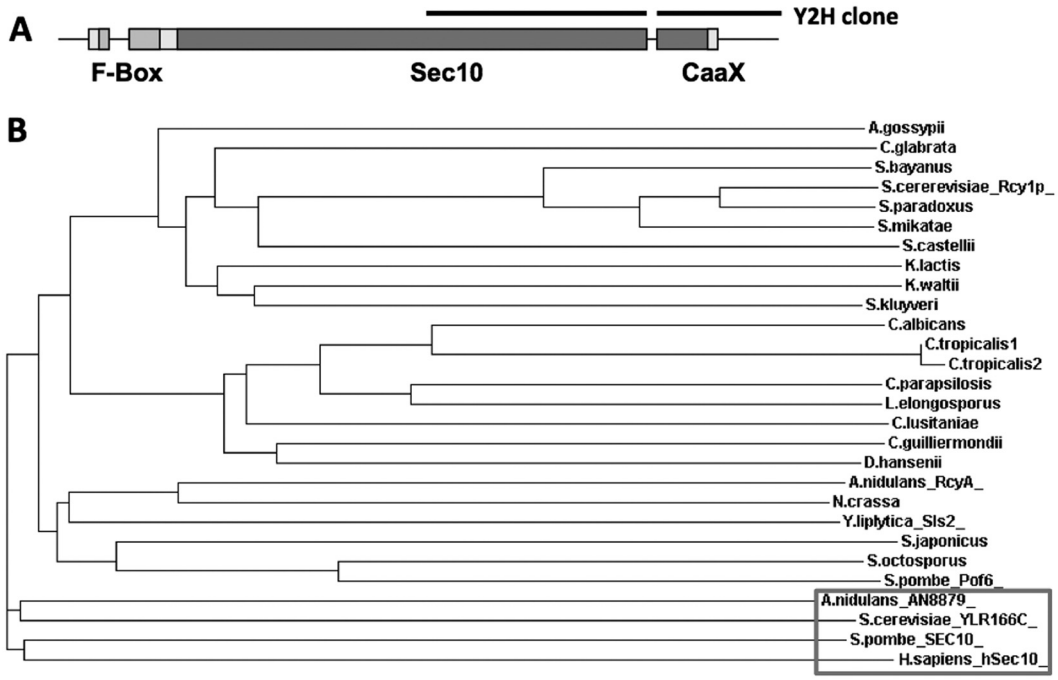

FIG 1 (A) Scheme of the RcyA protein. The F-box domain, the region with similarity to Sec10, and the CAAX motif are labeled. The original yeast two-hybrid (Y2H) clone is indicated above the scheme. (B) Relatedness analysis of RcyA. Fungal orthologues of RcyA and of Sec10 were aligned by tCoffee, and the tree was plotted at the EBI website (http://www.ebi.ac.uk/Tools/msa/tcoffee/). For the alignment, we used the Rcy1 orthologues of the following organisms: *Saccharomyces cerevisiae* (Rcy1p) (YJL204C), *Saccharomyces paradoxus* (spar343-g75.1), *Saccharomyces mikatae* (smik835-g3.1), *Saccharomyces bayanus* (sbayc610-g6.1), *Candida glabrata* (CAGL0F02497g), *Saccharomyces castellii* (Scas531.3), *Kluyveromyces waltii* (Kwal33.13585), *Kluyveromyces lactis* (KLLA0C03300g), *Saccharomyces kluyveri* (SAKL0C04004g), *Ashbya gossypii* (AFR644C), *Candida lusitaniae* (CLUG04919), *Debaryomyces hansenii* (DEHA2E19052g), *Candida guilliermondii* (PGUG03406.1), *Candida tropicalis1* (CTRG05296.3), *Candida tropicalis2* (CTRG06241.3), *Candida albicans* (orf19.3203), *Candida parapsilosis* (CPAG03322), *Lodderomyces elongisporus* (LELG03751), *Yarrowia lipolytica* (Sls2) (YALI0B19074g), *Aspergillus nidulans* (RcyA) (AN10061), *Neurospora crassa* (NCU03658), *Schizosaccharomyces japonicus* (SJAG02753), *Schizosaccharomyces octosporus* (SOCG02810), and *Schizosaccharomyces pombe* (Pof6) (SPCC18.04). In addition, we included the Se10 orthologues of the following organisms (boxed): *Saccharomyces cerevisiae* (YLR166C), *Aspergillus nidulans* (AN8879), *Schizosaccharomyces pombe* (SEC10) (SPAC13F5.06c), and *Homo sapiens* (hSec10) gi|24418661|sp|O00471.1|.

irreversibly to microtubules (26, 41, 42). In a strain expressing GFP-KipA^{rigor}, mRFP-RcyA did not colocalize along the microtubules decorated with GFP-KipA^{rigor} (Fig. 3B). These results indicate that KipA is not required for RcyA movement and distribution in the hyphae.

The dynamic behavior of GFP-RcyA around the hyphal tip resembled the movement of secretory vesicles. Therefore, we compared the localization of mRFP1-RcyA with that of GFP-SynA (v-SNARE) as a marker for such vesicles (Fig. 3C; see also Movie S2 in the supplemental material) (25). Since the fluorescent signal of secretory vesicles appeared to be very weak and since the vesicles moved very quickly, it was hard to document exact colocalization in movies, but their dynamic behaviors looked very similar. Besides that, SynA and RcyA colocalized at small dots at subapical regions, which might represent the late Golgi or trans-Golgi network (Fig. 3C, arrows) (43). Because conventional kinesin (kinesin-1) is involved in protein secretion, we hypothesized that KinA could be involved in RcyA movement (44–46). Indeed, mRFP-RcyA colocalized with GFP-KinA^{rigor} (Fig. 3D) (47). These results further suggest that RcyA is transported to the hyphal tip on secretory vesicles.

Because the bidirectional movement of RcyA at backward regions resembled the movement of early endosomes (26, 30), we compared the localization of mRFP1-RcyA with that of GFP-RabA (Rab GTPase) as a marker for early endosomes (Fig. 3E and F; see also Movie S2 in the supplemental material). However, colocalization of RabA and RcyA was hardly observed. Likewise, mRFP-RcyA colocalized only partially along microtubules decorated with GFP-UncA^{rigor} (Fig. 3G). UncA is involved in early endosome movement (15, 26). These results suggest that only a fraction of RcyA is transported along microtubules on early endosomes.

Deletion of *rcyA*. In order to determine the function of RcyA in *A. nidulans*, we created an *rcyA*-deletion strain. The *rcyA*-deletion strain grew as well as the wild type on agar plates, and no effect on conidiation or conidium density was observed (Fig. 4A). However, hyphae of the *rcyA*-deletion strain sometimes showed abnormal swellings, branch formation close to the tip, and split tips (Fig. 4B). The abnormal swellings around the tip were observed in 5% of the hyphae, and the tip split phenotype was observed in 1% of the hyphal tips ($n = 400$), but this phenotype was not observed in the wild type.

Because Rcy1 in *S. cerevisiae* is thought to be involved in membrane recycling but not in endocytosis, we tested whether the absence of RcyA in *A. nidulans* would affect membrane recycling. To this end, the membrane was stained with the fluorescent dye FM4-64 (36). Hyphae were incubated 15 min in the presence of the dye and then, after washing with media, immediately analyzed in the microscope at room temperature. The *rcyA*-deletion strain did not show obvious differences from the wild type in the internalization of FM4-64 (data not shown). When we treated the hy-

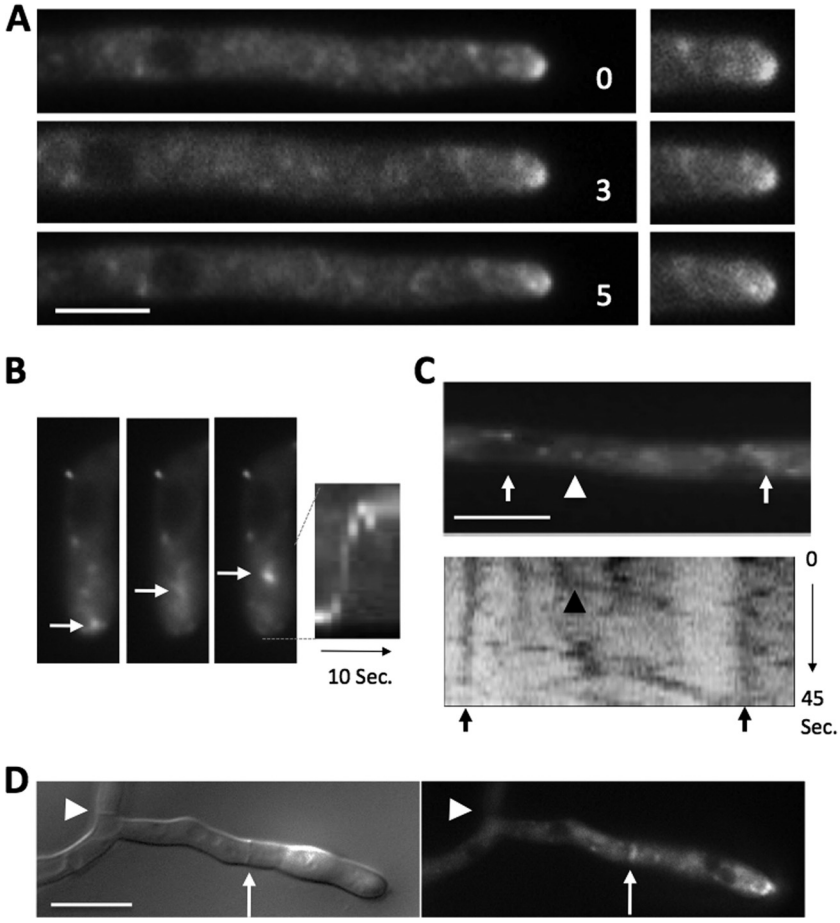

FIG 2 Localization of RcyA in *A. nidulans*. (A) GFP-RcyA was expressed under the control of the native promoter (SSH73). The elapsed time is given in seconds. (B) Time-lapse fluorescence microscopy images and the corresponding kymograph of the strain (SSH01). The three images correspond to three consecutive frames (300 ms each). The complete sequence spans 10 s. (C) A single picture of a time-lapse sequence of GFP-RcyA in strain SSH01 with the corresponding kymograph. The arrowheads indicate rapid moving RcyA spots. (D) Localization of mFRP1-RcyA at a forming septum (arrow) in the SSH54 strain. Strains with the RcyA construct under the control of the *alcA* promoter were grown with MM plus 2% glycerol in the medium. Scale bars represent 5 μm.

phae with the dye on ice for 15 min before microscopic analysis, the internalization of FM4-64 was partially delayed in the *rcyA*-deletion strain (data not shown). However, this could have been an indirect effect, given that the *rcy1* deletion caused a cold-sensitive phenotype in *S. cerevisiae* (10). Next, we tried to analyze membrane recycling, which means the transport of internalized dye from early endosomes back to the plasma membrane. It was hard to clearly visualize membrane recycling using this method, and no clear difference was observed in the numbers and sizes of early endosomes between the wild-type strain and the *rcyA*-deletion strain (data not shown).

Because *S. cerevisiae* Rcy1 is involved in v-SNARE Snc1 recycling, the localization of GFP-SynA (v-SNARE) was investigated in the *rcyA*-deletion strain (Fig. 4C). GFP-SynA localized at most hyphal tips without any obvious differences from the wild type (Fig. 4C, upper panel, and Fig. 3C), but accumulation of GFP-SynA was observed at subapical regions in abnormally swollen tips (Fig. 4C, lower panel).

Since the hyphae of the *rcyA*-deletion strain sometimes showed abnormal swellings or branch formation close to the tip, we investigated the localization of the two cell end markers TeaA and TeaR. Whereas both proteins were restricted to an area along the cytoplasmic membrane at the tip in the wild type, both proteins appeared less concentrated at the plasma membrane and localized at subapical swellings and also in the cytoplasm in the *rcyA*-deletion strain (Fig. 4D).

Overexpression of *rcyA*. If RcyA is involved in membrane recycling, we anticipated not only that downregulation of *rcyA* would disturb hyphal morphology but also that an increase of the concentration could affect hyphal growth and morphology. To test this hypothesis, the *alcA(p)-GFP-rcyA* construct was induced with threonine as the carbon source. The first obvious phenotypic changes were the much slower colony growth compared to the wild type and the lack of conidia (Fig. 5A). Under repressed conditions (with glucose as the carbon source), colonies grew as fast as the wild type. The expression level of GFP-RcyA under induced and repressed conditions was visible as the intensity of the GFP signal (Fig. 5B). Another phenotype concerned spore germination. *A. nidulans* conidia normally form a second germ tube at the side opposite the first one (Fig. 5C, left) (48). However, conidia of the *rcyA*-overexpression strain sometimes did not form second germ tubes (35%; $n = 100$) or formed a second germ tube at a random position (10%; $n = 100$). If there was a second germ tube, occasionally it appeared swollen (Fig. 5C, right).

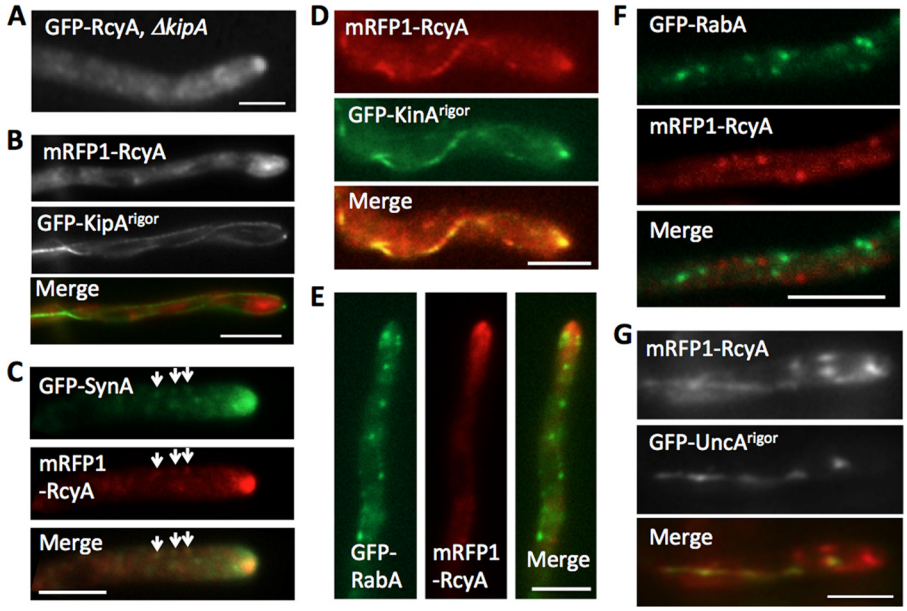

FIG 3 Transport of RcyA. (A) Fluorescence microscopy image of GFP-RcyA in *kipA*-deletion strain SSH08. (B) mRFP1-RcyA did not colocalize along the microtubule decorated with GFP-KipA^{rigor} in strain SSH66. (C) Colocalization of GFP-SynA (secretory vesicles) and mRFP1-RcyA in strain SSH56. (D) mRFP1-RcyA colocalized along the microtubule decorated with GFP-KinA^{rigor} in strain SSH91. (E and F) mRFP1-RcyA did not colocalize with GFP-RabA (early endosomes) around the hyphal tip (E) and backward region (F) in strain SSH93. (G) mRFP1-RcyA partially colocalized along the microtubule decorated with GFP-UncA^{rigor} in strain SSH55. Scale bars represent 5 μm.

RcyA controls the concentration of KipA. As described above, RcyA localization was independent of KipA. On the other hand, RcyA was isolated as a KipA-interacting protein. Therefore, we studied the role of this interaction. First, we confirmed the interaction using the bimolecular fluorescence complementation (BiFC) method. A bright signal close to the hyphal tip indicated that this interaction test result was positive (Fig. 6A).

In order to characterize the role of the two important motifs of RcyA, the CaaX motif and the F-box domain, we created strains in which the corresponding regions were deleted. When the CaaX motif was missing, no mRFP1 signal was observed at hyphal tips and forming seta but very weak staining of the cytoplasm was observed (Fig. 6B, data not shown). In contrast, deletion of the F-box domain of RcyA showed signal accumulation around the tips of hyphae (Fig. 6C). Other morphological features resembled the ones observed for the *rcyA* deletion.

S. cerevisiae Rcy1 was shown to control the turnover of several proteins (9). We hypothesized that *A. nidulans* RcyA could be involved in the turnover of KipA and thus that kinesin-7 could be a novel target for the F-box protein. In order to test this hypothesis, we compared the KipA concentration, as a GFP-KipA fusion protein, in an *rcyA*-deletion strain with the concentration in the wild type. GFP-KipA associates with the microtubule plus ends and appears as comet-like moving structures in the wild type (Fig. 6D, left) (24). In contrast, in the absence of RcyA, microtubules were evenly decorated (Fig. 6D, right). Such a decoration of the entire microtubule was also observed when KipA was overexpressed (24). This result suggested that the KipA protein concentration was higher in the *rcyA*-deletion strain than in the wild type. To further prove this hypothesis, the protein amount of GFP-KipA was determined by Western blot analysis (Fig. 6E). As a control, gamma-tubulin was chosen. Indeed, the KipA concentration was increased by about 50% in the *rcyA*-deletion strain in comparison to the wild type (Fig. 6E and F). Likewise, the KipA concentration was increased when only the F-box domain of RcyA was deleted (Fig. 6F). Because the *GFP-kipA* construct was expressed from the *alcA* promoter in both the wild-type strain and the Δ*rcyA* strain, an effect of RcyA on the transcription of *kipA* was unlikely. Indeed, the mRNA levels of *kipA* revealed no difference in the two strains (Fig. 6G). These results suggest that the RcyA interaction is necessary for the control of the KipA turnover and that RcyA is the specific adaptor for KipA in the ubiquitination and subsequent proteasome-degradation pathway.

DISCUSSION

The growth form of filamentous fungi requires massive membrane flow for the continuous extension of the plasma membrane at hyphal tips and the delivery of enzymes required for cell wall biosynthesis. Both are achieved through the fusion of secretory vesicles with the membrane at the growing tip. However, there is excellent evidence that endocytosis is also important for polar growth (12, 49). On the one hand, excess membrane can be removed through endocytosis. Likewise, a *slaB* mutant in which membrane internalization is inhibited shows massive invaginations of the membrane (50). SlaB is a key regulator of F-actin and the endocytic internalization machinery. Interestingly, deletion of the gene is lethal, showing the importance of endocytosis for polar growth. However, deletion of *rcyA* did not show any obvious severe morphological phenotypes or defects in the uptake of FM4-64. This is in agreement with the findings in *S. cerevisiae*, where only membrane recycling but not membrane internalization is disturbed in the *rcy1*-deletion strain (10).

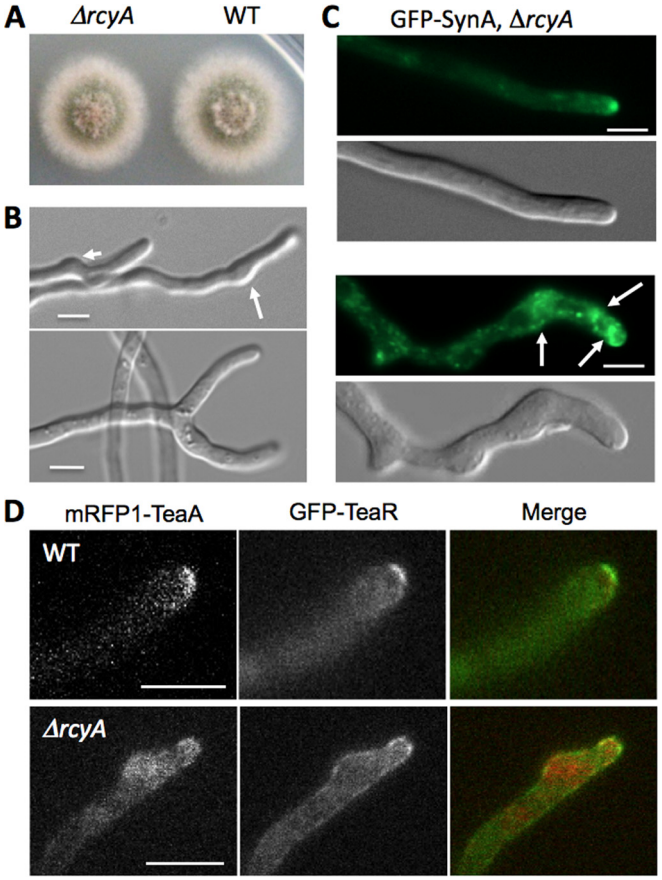

FIG 4 Deletion of *rcyA*. (A) Colonies of an *rcyA*-deletion strain (SSH36) and the wild-type (WT) strain (TN02A3) grown on MM with 2% glucose. Plates were incubated at 37°C for 48 h. (B) Swellings around the tips (arrows, upper) and the tip split phenotype (lower panel) in the *rcyA*-deletion strain. (C) Normal localization of GFP-SynA at most hyphal tips (upper panel) and accumulation of GFP-SynA at the subapical region of abnormally swollen tips in strain SSH89 (Δ*rcyA*) (lower panel). (D) Localization of the cell end markers mRFP1-TeaA and GFP-TeaR in the SNT56 (WT, upper panel) and SSH44 (Δ*rcyA*, lower panel) control strains. Scale bars represent 5 μm.

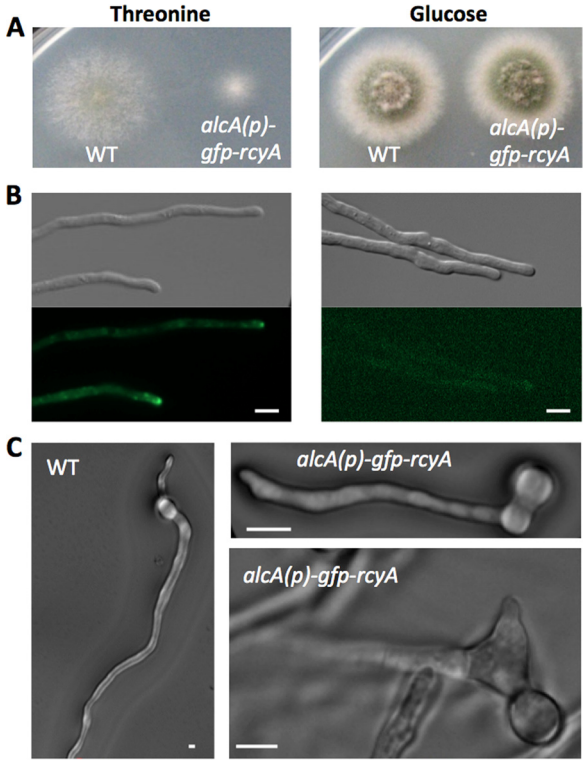

FIG 5 Overexpression of *rcyA*. (A) Colonies of the wild-type and SSH14 strains grown on MM plus 2% threonine (left) or MM plus 2% glucose (right). Plates were incubated at 37°C for 48 h. (B) Differential interference contrast (DIC) and GFP signal of SSH14 grown on MM plus 2% threonine (left) or MM plus 2% glucose (right). (C) DIC images of the wild-type and SSH14 germ tubes grown in MM plus 2% threonine. Scale bars represent 5 μm.

On the other hand, endocytosis actively occurs at a subapical ring of the hyphae and could contribute to the maintenance of polarity by recycling necessary components, such as cell end marker proteins (50). We found that the distribution of cell end marker proteins such as TeaR and TeaA in *A. nidulans* is impaired in the absence of RcyA. Since cell end marker proteins define the growth direction and are involved in branch formation, the misdistribution could be the reason for the observed changes in polar growth and branching in some minor fraction of the hyphae. Rcy1 in *S. cerevisiae* is thought to be involved in membrane recycling through the recycling of the v-SNARE Snc1 (8, 10). The v-SNARE SynA in *A. nidulans* occasionally accumulated at subapical regions in abnormally swollen tips (Fig. 4C, lower panel). This result supports the idea of a conserved function of RcyA with respect to SynA recycling; however, the defect of SynA recycling in the *rcyA*-deletion strain was only partial and appeared weaker than that of *S. cerevisiae*.

In comparison to the described role of *S. cerevisiae* Rcy1, Pof6 in *S. pombe* plays a critical role in cell separation, and gene deletion is lethal (9). We did not find any evidence for such a role in *A. nidulans*, although RcyA was found at septa. Of course, *A. nidulans* does not require cell separation and thus one would not expect a phenotype during vegetative growth. Since conidia are formed in a budding-like process, one would also not expect a phenotype corresponding to sporulation. However, one would expect a role of RcyA in filamentous fungi with a dimorphic switch between the filamentous form and a fission-yeast form, such as *Penicillium marneffei*.

Additionally, we identified KipA as a novel putative target for RcyA. The cellular concentration of KipA protein was increased upon deletion of the gene, while the gene expression level was comparable. We propose that RcyA is the E3 ubiquitin ligase adaptor responsible for the specific degradation of KipA in a SCF complex and that RcyA is necessary for the control of the KipA turnover. Here we cannot exclude the possibility that the increase of KipA protein levels in the *rcyA*-deletion strain is due to translational control. To exclude this possibility, the half-life time of KipA needs to be investigated. The overexpression of *rcyA* did not reduce the KipA concentration significantly and did not phenocopy the *kipA*-deletion phenotype (data not shown), suggesting that the residual KipA amount is sufficient. However, there is some similarity between the *kipA*-deletion phenotype and the *rcyA*-deletion phenotype, because both deletions disturb cell end marker organization. Nevertheless, TeaR was scattered along the plasma membrane in the *rcyA*-deletion strain, whereas it was organized in a compact structure in the *kipA*-deletion strain. This

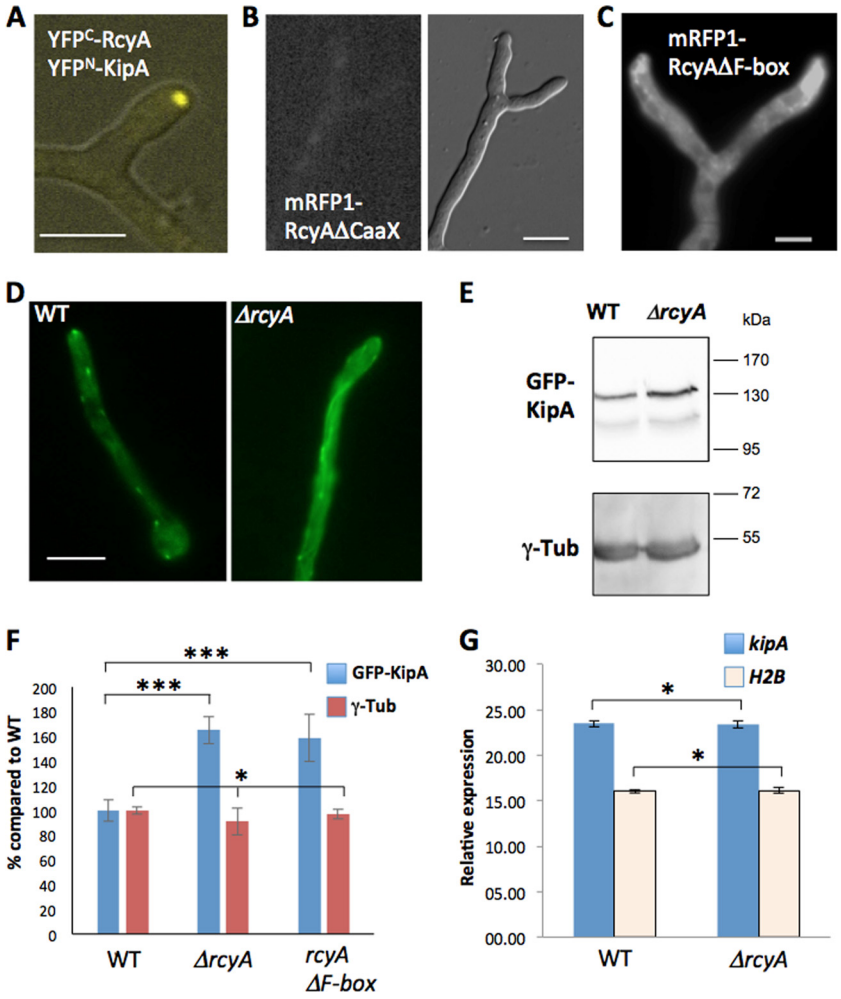

FIG 6 Effect of *rcyA* deletion on the KipA concentration. (A) Bimolecular fluorescence complementation of RcyA and KipA. (B and C) Localization of mRFP1-RcyA-deleted CaaX motif (B) and mRFP1-RcyA-deleted F-box (C). (D) Localization of GFP-KipA in the wild-type (SSH27) and SSH43 (Δ*rcyA*) strains. The microscopy medium was MM plus 2% glycerol. (E) Western blotting of cell lysate, SSH27 (GFP-KipA), SSH43 (GFP-KipA, Δ*rcyA*), and SSH69 (GFP-KipA, mRFP1-RcyAΔF-box) (strain SSH69 is not shown here), using a polyclonal anti-GFP antibody and a monoclonal anti-gamma-tubulin (γ-Tub) antibody as an internal control for the basal protein amount. (F) Relative levels of GFP-KipA and gamma-tubulin in the Western blotting. The wild-type value was set to 100% ($n = 6$). *, $P > 0.05$ (no significant difference); ***, $P > 0.001$ (highly significant difference). (G) Expression of the *kipA* gene. The graph represents the relative levels of expression of the *kipA* gene as measured by RT-PCR. *H2B* was used as a control. All experiments were done with three biological and two technical replicates. Scale bars represent 5 μm.

difference might be explained if we assume that membrane recycling is unaffected in the *kipA*-deletion strain but disturbed in the absence of RcyA. Taken together, our results are further evidence for a role of the endocytic ring in polarity maintenance and the importance of endocytosis in polar growth.

ACKNOWLEDGMENTS

This work was supported by the German Science Foundation (DFG) Research Unit (FOR1334). N.T. was a Humboldt Fellow.

REFERENCES

1. **Peters JM.** 1998. SCF and APC: the yin and yang of cell cycle regulated proteolysis. Curr. Opin. Cell Biol. **10:**759–768. http://dx.doi.org/10.1016/S0955-0674(98)80119-1.
2. **Krappmann S, Jung N, Medic B, Busch S, Prade RA, Braus GH.** 2006. The *Aspergillus nidulans* F-box protein GrrA links SCF activity to meiosis. Mol. Microbiol. **61:**76–88. http://dx.doi.org/10.1111/j.1365-2958.2006.05215.x.
3. **von Zeska Kress MR, Harting R, Bayram ¨O, Christmann M, Irmer H, Valerius O, Schinke J, Goldman GH, Braus GH.** 2012. The COP9 signalosome counteracts the accumulation of cullin SCF ubiquitin E3 RING ligases during fungal development. Mol. Microbiol. **83:**1162–1177. http://dx.doi.org/10.1111/j.1365-2958.2012.07999.x.
4. **Colabardini AC, Humanes AC, Gouvea PF, Savoldi M, Goldman MH, Kress MR, Bayram Ö, Oliveira JV, Gomes MD, Braus GH, Goldman GH.** 2012. Molecular characterization of the *Aspergillus nidulans fbxA* encoding an F-box protein involved in xylanase induction. Fungal Genet. Biol. **49:**130–140. http://dx.doi.org/10.1016/j.fgb.2011.11.004.
5. **Schnell JD, Hicke L.** 2003. Non-traditional functions of ubiquitin and ubiquitin-binding proteins. J. Biol. Chem. **278:**35857–35860. http://dx.doi.org/10.1074/jbc.R300018200.
6. **Wiederkehr A, Avaro S, Prescianotto-Baschong C, Haguenauer-Tsapis R, Riezman H.** 2000. The F-box protein Rcy1p is involved in endocytic membrane traffic and recycling out of an early endosome in *Saccharomyces cerevisiae*. J. Cell Biol. **149:**397–410. http://dx.doi.org/10.1083/jcb.149.2.397.
7. **Furuta N, Fujimura-Kamada K, Saito K, Yamamoto T, Tanaka K.** 2007. Endocytic recycling in yeast is regulated by putative phospholipid trans-

locases and the Ypt31/32p-Rcy1p pathway. Mol. Biol. Cell **18:**295–312. http://dx.doi.org/10.1091/mbc.E06-05-0461.
8. **Chen SH, Chen S, Tokarev AA, Liu F, Jedd G, Segev N.** 2005. Ypt31/32 GTPases and their novel F-box effector protein Rcy1 regulate protein recycling. Mol. Biol. Cell **16:**178–192. http://dx.doi.org/10.1091/mbc.E04-03-0258.
9. **Hermand D, Bamps S, Tafforeaus L, Vandenhaute J, Mäkelä TP.** 2003. Skp1 and the F-box protein Pof6 are essential for cell separation in fission yeast. J. Biol. Chem. **278:**9671–9677. http://dx.doi.org/10.1074/jbc.M211358200.
10. **Chen SH, Shah AH, Segev N.** 2011. Ypt31/32 GTPases and their F-box effector Rcy1 regulated ubiquitination of recycling proteins. Cell Logist. **1:**21–31. http://dx.doi.org/10.4161/cl.1.1.14695.
11. **Riquelme M, Yarden O, Bartnicki-Garcia S, Bowman B, Castro-Longoria E, Free SJ, Fleissner A, Freitag M, Lew RR, Mouriño-Pérez R, Plamann M, Rasmussen C, Richthammer C, Roberson R-W, Sanchez-Leon E, Seiler S, Watters MK.** 2011. Architecture and development of the *Neurospora crassa* hypha - a model cell for polarized growth. Fungal Biol. **115:**446–474. http://dx.doi.org/10.1016/j.funbio.2011.02.008.
12. **Steinberg G.** 14 May 2014. Endocytosis and early endosome motility in filamentous fungi. Curr. Opin. Microbiol. http://dx.doi.org/10.1016/j.mib.2014.04.001.
13. **Peñalva MA.** 2010. Endocytosis in filamentous fungi: Cinderella gets her reward. Curr. Opin. Microbiol. **13:**684–692. http://dx.doi.org/10.1016/j.mib.2010.09.005.
14. **Peñalva MA, Galindo A, Abenza JF, Pinar M, Cacagno-Pizarelli AM, Arst HN, Pantazopoulou A.** 2012. Searching for gold beyond mitosis: mining intracellular membrane traffic in *Aspergillus nidulans*. Cell Logist. **2:**2–14. http://dx.doi.org/10.4161/cl.19304.
15. **Seidel C, Moreno-Velásquez SD, Riquelme M, Fischer R.** 2013. *Neurospora crassa* NKIN2, a kinesin-3 motor, transports early endosomes and is required for polarized growth. Eukaryot. Cell **12:**1020–1032. http://dx.doi.org/10.1128/EC.00081-13.
16. **Fischer R, Zekert N, Takeshita N.** 2008. Polarized growth in fungi - interplay between the cytoskeleton, positional markers and membrane domains. Mol. Microbiol. **68:**813–826. http://dx.doi.org/10.1111/j.1365-2958.2008.06193.x.
17. **Takeshita N, Manck R, Grün N, de Vega S, Fischer R.** 27 May 2014. Interdependence of the actin and the microtubule cytoskeleton during fungal growth. Curr. Opin. Microbiol. http://dx.doi.org/10.1016/j.mib.2014.04.005.
18. **Mata J, Nurse P.** 1997. *tea1* and the microtubular cytoskeleton are important for generating global spatial order within the fission yeast cell. Cell **89:**939–949. http://dx.doi.org/10.1016/S0092-8674(00)80279-2.
19. **Takeshita N, Higashitsuji Y, Konzack S, Fischer R.** 2008. Apical sterol-rich membranes are essential for localizing cell end markers that determine growth directionality in the filamentous fungus *Aspergillus nidulans*. Mol. Biol. Cell **19:**339–351. http://dx.doi.org/10.1091/mbc.E07-06-0523.
20. **Takeshita N, Mania D, Herrero S, Ishitsuka Y, Nienhaus GU, Podolski M, Howard J, Fischer R.** 2013. The cell-end marker TeaA and the microtubule polymerase AlpA contribute to microtubule guidance at the hyphal tip cortex of *Aspergillus nidulans* to provide polarity maintenance. J. Cell Sci. **126:**5400–5411. http://dx.doi.org/10.1242/jcs.129841.
21. **Hill TW, Käfer E.** 2001. Improved protocols for *Aspergillus* minimal medium: trace element and minimal medium salt stock solutions. Fungal Genet. Newsl. **48:**20–21.
22. **Nayak T, Szewczyk E, Oakley CE, Osmani A, Ukil L, Murray SL, Hynes MJ, Osmani SA, Oakley BR.** 2006. A versatile and efficient gene targeting system for *Aspergillus nidulans*. Genetics **172:**1557–1566. http://dx.doi.org/10.1534/genetics.105.052563.
23. **Stringer MA, Dean RA, Sewall TC, Timberlake WE.** 1991. *Rodletless*, a new *Aspergillus* developmental mutant induced by directed gene inactivation. Genes Dev. **5:**1161–1171. http://dx.doi.org/10.1101/gad.5.7.1161.
24. **Konzack S, Rischitor P, Enke C, Fischer R.** 2005. The role of the kinesin motor KipA in microtubule organization and polarized growth of *Aspergillus nidulans*. Mol. Biol. Cell **16:**497–506. http://dx.doi.org/10.1091/mbc.E04-02-0083.
25. **Taheri-Talesh N, Horio T, Araujo-Bazan L, Dou X, Espeso EA, Penalva MA, Osmani A, Oakley BR.** 2008. The tip growth apparatus of *Aspergillus nidulans*. Mol. Biol. Cell **19:**1439–1449. http://dx.doi.org/10.1091/mbc.E07-05-0464.
26. **Zekert N, Fischer R.** 2009. The *Aspergillus nidulans* kinesin-3 UncA motor moves vesicles along a subpopulation of microtubules. Mol. Biol. Cell **20:**673–684. http://dx.doi.org/10.1091/mbc.E08-07-0685.
27. **Herrero S, Takeshita N, Fischer R.** 2011. The *Aspergillus nidulans* CENP-E kinesin motor KipA interacts with the fungal homologue of the centromere-associated protein CENP-H at the kinetochore. Mol. Microbiol. **80:**981–994. http://dx.doi.org/10.1111/j.1365-2958.2011.07624.x.
28. **Efimov V, Zhang J, Xiang X.** 2006. CLIP-170 homologue and NUDE play overlapping roles in NUDF localization in *Aspergillus nidulans*. Mol. Biol. Cell **17:**2021–2034. http://dx.doi.org/10.1091/mbc.E05-11-1084.
29. **Veith D, Scherr N, Efimov VP, Fischer R.** 2005. Role of the spindle-pole body protein ApsB and the cortex protein ApsA in microtubule organization and nuclear migration in *Aspergillus nidulans*. J. Cell Sci. **118:**3705–3716. http://dx.doi.org/10.1242/jcs.02501.
30. **Abenza JF, Pantazopoulou A, Rodríguez JM, Galindo A, Peñalva MA.** 2009. Long-distance movement of *Aspergillus nidulans* early endosomes on microtubule tracks. Traffic **10:**57–75. http://dx.doi.org/10.1111/j.1600-0854.2008.00848.x.
31. **Yelton MM, Hamer JE, Timberlake WE.** 1984. Transformation of *Aspergillus nidulans* by using a *trpC* plasmid. Proc. Natl. Acad. Sci. U. S. A. **81:**1470–1474. http://dx.doi.org/10.1073/pnas.81.5.1470.
32. **Sambrook J, Russel DW.** 1999. Molecular cloning: a laboratory manual. Cold Spring Harbor Laboratory Press, Cold Spring Harbor, NY.
33. **Szewczyk E, Nayak T, Oakley CE, Edgerton H, Xiong Y, Taheri-Talesh N, Osmani SA, Oakley BR.** 2006. Fusion PCR and gene targeting in *Aspergillus nidulans*. Nat. Protoc. **1:**3111–3120. http://dx.doi.org/10.1038/nprot.2006.405.
34. **Osmani A, Oakley BR, Osmani SA.** 2006. Identification and analysis of essential *Aspergillus nidulans* genes using the heterokaryon rescue technique. Nat. Protoc. **1:**2517–2526. http://dx.doi.org/10.1038/nprot.2006.406.
35. **Waring RB, May GS, Morris NR.** 1989. Characterization of an inducible expression system in *Aspergillus nidulans* using *alcA* and tubulin coding genes. Gene **79:**119–130. http://dx.doi.org/10.1016/0378-1119(89)90097-8.
36. **Peñalva MA.** 2005. Tracing the endocytic pathway of *Aspergillus nidulans* with FM4-64. Fungal Genet. Biol. **42:**963–975. http://dx.doi.org/10.1016/j.fgb.2005.09.004.
37. **Boisramé A, Beckerich JM, Gaillardin C.** 1999. A mutation in the secretion pathway of the yeast *Yarrowia lipolytica* that displays synthetic lethality in combination with a mutation affecting the signal recognition particle. Mol. Gen. Genet. **261:**601–609. http://dx.doi.org/10.1007/s004380050002.
38. **Galan JM, Wiederkehr A, Seol JH, Haguenauer-Tsapis R, Deshaies RJ, Riezman H, Peter M.** 2001. Skp1p and the F-box protein Rcy1p form a non-SCF complex involved in recycling of the SNARE Snc1p in yeast. Mol. Cell. Biol. **21:**3105–3117. http://dx.doi.org/10.1128/MCB.21.9.3105-3117.2001.
39. **Guo W, Roth D, Gatt E, Novick P.** 1997. Identification and characterization of homologues of the exocyst component Sec10p. FEBS Lett. **404:**135–139. http://dx.doi.org/10.1016/S0014-5793(97)00109-9.
40. **Elias 1, Drdova E, Ziak D, Bavlnka B, Hala M, Cvrckova F, Soukupova H, Zarsky V.** 2003. The exocyst complex in plants. Cell Biol. Int. **27:**199–201. http://dx.doi.org/10.1016/S1065-6995(02)00349-9.
41. **Meluh PB, Rose MD.** 1990. *KAR3*, a kinesin-related gene required for yeast nuclear fusion. Cell **60:**1029–1041. http://dx.doi.org/10.1016/0092-8674(90)90351-E.
42. **Nakata T, Hirokawa N.** 1995. Point mutation of adenosine triphosphate-binding motif generated rigor kinesin that selectively blocks anterograde lysosome membrane transport. J. Cell Biol. **131:**1039–1053. http://dx.doi.org/10.1083/jcb.131.4.1039.
43. **Pinar M, Pantazopoulou A, Arst HN, Peñalva MA.** 2013. Acute inactivation of the *Aspergillus nidulans* Golgi membrane fusion machinery: correlation of apical extension arrest and tip swelling with cisternal disorganization. Mol. Microbiol. **89:**228–248. http://dx.doi.org/10.1111/mmi.12280.
44. **Seiler S, Nargang FE, Steinberg G, Schliwa M.** 1997. Kinesin is essential for cell morphogenesis and polarized secretion in *Neurospora crassa*. EMBO J. **16:**3025–3034. http://dx.doi.org/10.1093/emboj/16.11.3025.
45. **Schuster M, Treitschke S, Kilaru S, Molloy J, Harmer NJ, Steinberg G.** 2012. Myosin-5, kinesin-1 and myosin-17 cooperate in secretion of fungal chitin synthase. EMBO J. **31:**214–227. http://dx.doi.org/10.1038/emboj.2011.361.

46. **Requena N, Alberti-Segui C, Winzenburg E, Horn C, Schliwa M, Philippsen P, Liese R, Fischer R.** 2001. Genetic evidence for a microtubule-destabilizing effect of conventional kinesin and analysis of its consequences for the control of nuclear distribution in *Aspergillus nidulans*. Mol. Microbiol. **42:**121–132. http://dx.doi.org/10.1046/j.1365-2958.2001.02609.x.
47. **Seidel C, Zekert N, Fischer R.** 2012. The *Aspergillus nidulans* kinesin-3 tail is necessary and sufficient to recognize modified microtubules. PLoS One **7:**e30976. http://dx.doi.org/10.1371/journal.pone.0030976.
48. **Takeshita N, Fischer R.** 2011. On the role of microtubules, cell end markers, and septal microtubule organizing centers on site selection for polar growth in *Aspergillus nidulans*. Fungal Biol. **115:**506–517. http://dx.doi.org/10.1016/j.funbio.2011.02.009.
49. **Valdez-Taubas J, Pelham HR.** 2003. Slow diffusion of protein in the yeast plasma membrane allows polarity to be maintained by endocytic cycling. Curr. Biol. **13:**1636–1640. http://dx.doi.org/10.1016/j.cub.2003.09.001.
50. **Araujo-Bazán L, Peñalva MA, Espeso EA.** 2008. Preferential localization of the endocytic internalization machinery to hyphal tips underlies polarization of the actin cytoskeleton in *Aspergillus nidulans*. Mol. Microbiol. **67:**891–905. http://dx.doi.org/10.1111/j.1365-2958.2007.06102.x.